



Timing and magnitude of early to middle Holocene warming in East Greenland inferred from chironomids

Journal:	<i>Boreas</i>
Manuscript ID	BOR-059-2016.R2
Manuscript Type:	Original Article
Date Submitted by the Author:	n/a
Complete List of Authors:	Axford, Yarrow; Northwestern University, Dept. of Earth and Planetary Sciences Levy, Laura; Department of Geoscience, Aarhus University Kelly, Meredith A.; Dartmouth College, Earth Sciences Francis, Donna; Department of Geosciences, University of Massachusetts Hall, Brenda; University of Maine, School of Earth Sciences and the Climate Change Langdon, Peter G.; University of Southampton, Geography Lowell, Thomas; University of Cincinnati, Geology
Keywords:	Arctic, Greenland, Chironomidae, midges, Holocene Thermal Maximum, paleotemperatures, paleolimnology, lake sediments

1
2
3
4
5
6
7
8
9
10
11
12
13
14
15
16
17
18
19
20
21
22
23
24
25
26
27
28
29
30
31
32
33
34
35
36
37
38
39
40
41
42
43
44
45
46
47
48
49
50
51
52
53
54
55
56
57
58
59
60

1 Timing and magnitude of early to middle Holocene warming in East Greenland
2 inferred from chironomids

3
4 YARROW AXFORD, LAURA B. LEVY, MEREDITH A. KELLY, DONNA R. FRANCIS,
5 BRENDA L. HALL, PETER G. LANGDON AND THOMAS V. LOWELL

6
7
8 Axford, Y., Levy, L. B., Kelly, M. A., Francis, D. R., Hall, B. L., Langdon, P. G. & Lowell, T.
9 V.: Timing and magnitude of early to middle Holocene warming in East Greenland inferred from
10 chironomids.

11

12 Much of Greenland experienced summers warmer than present during parts of the early to
13 middle Holocene, during a precession-driven positive anomaly in summer insolation. However,
14 the magnitude of that warmth remains poorly known, and its timing and spatial pattern are
15 uncertain. Here we describe the first quantitative Holocene palaeotemperature reconstruction
16 from central East Greenland based upon insect (chironomid) assemblages preserved in lake
17 sediments. We postulate that landscapes like our study site, characterized by minimal soil and
18 vegetation development through the Holocene and thus less influenced by some important
19 secondary gradients, are especially well-suited to the use of chironomids to reconstruct Holocene
20 temperatures. The inferred timing of warmth at our study site near Scoresby Sund agrees well
21 with other nearby evidence, including glacial geological reconstructions and temperatures
22 inferred from precipitation isotopes at Renland ice cap, supporting the use of chironomids to
23 reconstruct temperatures at this site. We infer highest temperatures from ~10 to 5.5 ka, followed
24 by gradual cooling after 5.5 ka and progressively colder and less productive conditions after 3.5
25 ka. Models based upon two independent training sets yield similar inferred temperature trends,
26 and suggest an average summer temperature anomaly from ~10 to 5.5 ka of 3 to 4 °C relative to
27 the preindustrial last millennium. The estimated overall rate of Neoglacial cooling averaged over
28 the period from 5.5 to 0.5 ka was 0.6 to 0.8 °C per thousand years, more than twice the rate

1
2
3 29 previously estimated for the Arctic as a whole. Given strong apparent spatial variability in
4
5 30 Holocene climate around the Arctic, and the utility of palaeoclimate data for improving climate
6
7
8 31 and ice sheet models, it should be a priority to further quantify past temperature changes around
9
10 32 the margins of the Greenland Ice Sheet, where few quantitative reconstructions exist and future
11
12
13 33 warming will affect global sea level.
14

15 34
16 35 *Yarrow Axford (axford@northwestern.edu), Department of Earth and Planetary Sciences, Northwestern University,*
17 36 *Evanston, IL, USA 60208; Laura B. Levy, Department of Geoscience, Aarhus University, 8000 Aarhus C, Denmark;*
18 37 *Meredith A. Kelly, Department of Earth Sciences, Dartmouth College, Hanover, NH, USA 03750; Donna R.*
19 38 *Francis, Department of Geosciences, University of Massachusetts, 233 Morrill Science Center, Amherst, MA, USA*
20 39 *01003; Brenda L. Hall, School of Earth and Climate Sciences and the Climate Change Institute, University of*
21 40 *Maine, Orono, ME, USA 04469; Peter G. Langdon, Geography and Environment, University of Southampton,*
22 41 *Highfield, Southampton SO17 1BJ UK; Thomas V. Lowell, Department of Geology, University of Cincinnati,*
23 42 *Cincinnati, OH, USA 45221.*
24 43

Review Only

1
2
3
4
5
6
7
8
9
10
11
12
13
14
15
16
17
18
19
20
21
22
23
24
25
26
27
28
29
30
31
32
33
34
35
36
37
38
39
40
41
42
43
44
45
46
47
48
49
50
51
52
53
54
55
56
57
58
59
60

Diverse palaeoenvironmental records from Greenland’s ice-free margin and surrounding seas record very different conditions during the late Holocene than in the early to middle Holocene, when enhanced summer insolation drove higher summer temperatures. During the Holocene Thermal Maximum (HTM), thermophilous species migrated north and glaciers and sea ice were less extensive in many sectors of Greenland (e.g., Kaufman *et al.* 2004; Funder *et al.* 2011; Larsen *et al.* 2015; Briner *et al.* 2016). These environmental responses to HTM warming hold clues to what the future impacts of anthropogenic warming around Greenland are likely to be – including changes in the Greenland Ice Sheet and thus global sea level. However, such assessments are currently hampered by uncertainties regarding the magnitude and spatiotemporal pattern of HTM warmth over Greenland (Lecavalier *et al.* 2014).

Most quantitative estimates of the HTM temperature anomaly over Greenland thus far come from the Greenland Ice Sheet itself (Dahl-Jensen *et al.* 1998; Johnsen *et al.* 2001; Vinther *et al.* 2009; Sundqvist *et al.* 2014), a perspective limited to high-elevation conditions over ice, some of which experienced large elevation changes through the Holocene (Vinther *et al.* 2009). A small but growing database of quantitative palaeotemperature reconstructions from Greenland lakes is adding alternative perspectives (Fréchette & de Vernal 2009; D’Andrea *et al.* 2011; Axford *et al.* 2013; Gajewski 2015).

Subfossil chironomid (Insecta: Diptera: Chironomidae, or non-biting midge) assemblages preserved in lake sediments are increasingly used across the Arctic and subarctic to reconstruct Holocene temperatures, as indicated for example by the proxy’s representation in recent reviews of Holocene climate records by Briner *et al.* (2016) and Kaufman *et al.* (2016). Studies of chironomid assemblages in surface sediments along spatial and climatic transects have repeatedly demonstrated that temperature is a dominant predictor of chironomid species

distributions (e.g., Walker *et al.* 1991; Eggermont & Heiri 2011; Fortin *et al.* 2015), and chironomid remains are nearly ubiquitous and often abundant in the Arctic's many small non-glacial lakes. Pioneering qualitative palaeoclimate interpretations from chironomid assemblages have been published at several sites in eastern and northeastern Greenland (Wagner *et al.* 2005; Schmidt *et al.* 2011; Wagner & Bennike 2015). However, quantitative chironomid-based temperature reconstructions have previously been published from only two sites on Greenland, both on the island's west coast and in warmer climates than that of our current study site (Wooller *et al.* 2004; Axford *et al.* 2013).

Here we describe a new quantitative reconstruction of temperature shifts through the Holocene from insect remains preserved in sediments of a lake in central East Greenland near Scoresby Sund and Renland ice cap (Fig. 1). Bulk sedimentological data from the same lake sediment cores were previously presented by Levy *et al.* (2014), who combined geomorphic mapping and cosmogenic surface exposure dating with analysis of lake sediment records to reconstruct fluctuations of nearby Bregne ice cap through the Holocene. We build upon that work by developing a proxy-based climate reconstruction for the region that is independent of glacier behavior.

Study site and methods

Last Chance Lake (informal name; hereafter LCL) is a small (8.9 m deep, 0.007 km²) non-glacial lake located at 70.90645 °N 25.56945 °W and 660 m a.s.l. on Milne Land, 60 km southeast of Renland ice cap and 5 km from the coastline of inner Scoresby Sund (Figs 1, 2). The lake is almost 110 km from the nearest small settlement, Nerlerit Inaat airport at Constable Point, and

1
2
3
4
5
6
7
8
9
10
11
12
13
14
15
16
17
18
19
20
21
22
23
24
25
26
27
28
29
30
31
32
33
34
35
36
37
38
39
40
41
42
43
44
45
46
47
48
49
50
51
52
53
54
55
56
57
58
59
60

thus remote from direct human impacts. LCL has been isolated from glacial meltwater since its catchment was deglaciated by 10.7 ka (Levy *et al.* 2014; ka = thousands of calibrated years BP). It has seasonal surface inflow and outflow today, and is surrounded by very sparsely vegetated boulder fields (Fig. 2). Surface water temperature in LCL was 8.8 °C on September 5, 2010. Regional climate is strongly influenced by cold surface waters and frequent pack ice off the outer coast, associated with the East Greenland Current. At Ittoqqortoormiit, 140 km to the east at 65 m a.s.l. on the outer coast, mean July temperature is 7.1 °C and mean annual temperature is -6.1 °C for recent years (AD 1986-2011; Carstensen & Jørgensen 2009).

As described by Levy *et al.* (2014), three overlapping piston cores capture the modern sediment-water interface and the entire Holocene package of 75.5 cm of laminated/stratified lacustrine mud overlying 8 cm of basal diamicton, the latter interpreted as till dating to regional deglaciation. For the current study, the ten AMS ¹⁴C ages reported by Levy *et al.* (2014) on aquatic plants or invertebrates from the lacustrine sediment unit were re-calibrated (updated) based upon the IntCal13 curve (Reimer *et al.* 2013). We conducted age-depth modelling using the freely available software *clam* version 2.2 (Blaauw 2010), with all ages from the lacustrine mud unit equally weighted. Like Levy *et al.* (2014), we excluded two inverted ages obtained on aquatic plants recovered from the basal diamicton which we speculate were dragged down the edges of the tube during coring. Because an intact sediment-water interface was recovered, 0 cm depth was assigned a modern age (AD 2010, the year of sample collection). All ages before ~10 ka are extrapolated beneath the lowest ¹⁴C sample, thus very uncertain. We do not extrapolate beyond the base of the lacustrine unit at 75.5 cm depth. Throughout this paper, we subdivide the Holocene according to the suggestions of Walker *et al.* (2012), who define the middle Holocene as bounded between 8.2 and 4.2 ka.

Weight percent organic matter (OM) in bulk sediment was estimated by loss-on-ignition at 550 °C for two hours (Heiri *et al.* 2001). Weight percent biogenic silica (bioSiO₂) was measured following the methods described by Mortlock & Froelich (1989), using 10% Na₂CO₃. Chironomid (Diptera: Chironomidae) remains >100 µm were analyzed following standard protocols (Walker 2001). Between 52 and 215 whole head capsules were identified per sample (median count sum was 109 whole head capsules), except for three samples processed from below the lacustrine unit (i.e., within the diamicton) which yielded no head capsules. Sample sizes ranged from 0.1 to 0.5 g dry sediment for all except the sample at 75 cm depth (the deepest sample to yield any head capsules, with low head capsule concentrations that necessitated a sample size of 3.9 g). Head capsules were identified with reference to Wiederholm (1983) and Brooks *et al.* (2007). We identified one unknown morphotype as *Psectrocladius nr barbimanus* type. *P. nr barbimanus* type appears similar to *P. barbimanus* type (Brooks *et al.* 2007) but with sharply angular median and first lateral teeth, and with median teeth that may have a small apical projection and that are at least as tall as the first lateral teeth (Fig. 3).

July air temperatures were modeled using two transfer functions with independent training sets: One, a weighted-averaging (WA) model with inverse deshrinking and tolerance downweighting, based upon a northeastern North American training set including 68 sites representing a July air temperature gradient of 5.0 to 19.0 °C and spanning from the Canadian Arctic islands west of Greenland to Maine, USA (Francis *et al.* 2006; 44 taxa, $r^2_{\text{jack}} = 0.88$, RMSEP = 1.5 °C; hereafter FRA06). Two, a two-component WA partial-least-squares (WA-PLS) model employing a large northern North American training set, comprising 434 sites representing a July air temperature gradient from 2.0 to 16.3 °C and spanning from Alaska, USA to eastern Canada and from Boreal to High Arctic environments, including the Canadian Arctic

1
2
3
4
5
6
7
8
9
10
11
12
13
14
15
16
17
18
19
20
21
22
23
24
25
26
27
28
29
30
31
32
33
34
35
36
37
38
39
40
41
42
43
44
45
46
47
48
49
50
51
52
53
54
55
56
57
58
59
60

islands (Fortin *et al.* 2015; 78 taxa, $r^2_{boot} = 0.72$, RMSEP = 1.9 °C; hereafter FOR15). Neither training set contains calibration data from East Greenland, and no chironomid training set yet exists for East Greenland or any other Mid- to High Arctic sector of Greenland. The Francis *et al.* (2006) training set was used in a previous Holocene study in warmer West Greenland (Axford *et al.* 2013). Fossil assemblages in East Greenland have much in common with assemblages from the Canadian Arctic at the genus level (Gajewski *et al.* 2005; Francis *et al.* 2006; Fortin *et al.* 2015), but we did find some differences at the sub-genus level, e.g. within *Psectrocladius*. To assess the similarity of modern analogues to our fossil assemblages, we used the modern analogue technique (MAT) and calculated squared chord distances (SCDs) between each untransformed fossil assemblage and its closest modern analogue in each training set.

Palaeotemperatures were modeled on square-root transformed species data using C2 v. 1.7.6. Most subfossil morphotypes identified to species type level, e.g., the morphotypes of *Cricotopus/Orthocladius* and *Psectrocladius* (*Psectrocladius*), were lumped at the genus level to harmonize with the training sets. All subfossil taxa were utilized in temperature modelling, except two minor taxa that are absent or excluded from both models: *Trissocladius* (which is absent from both training sets but occurs in six downcore samples at a maximum abundance of three percent) and *Diamesa* (of which two head capsules were found in our bottommost gyttja sample). The mix of *Psectrocladius* species types lumped in the FRA06 training set is not described, but we know that the training set includes *P. sordidellus* type, whereas *P. barbimanus* and *P. nr barbimanus* types are most abundant at our study site. In the FRA06 training set, the Tanypodinae are also mostly undifferentiated and (given the broad climate gradient of the training set sites) likely to include a different mix of species types than our cold, Mid- to High-Arctic study site. As a means to assess our reconstruction's sensitivity to possible taxonomic

159 differences between our study site and the training set sites, temperature modelling was
160 performed both with and without these two groups using the FRA06 training set.

161

162 **Results**

163

164 *Chronology*

165 A smooth spline age model (error-weighted, with smoothness parameter = 0.4) was used to
166 estimate age-depth relationships down core (Fig. 4). Our updated age model is entirely within
167 model error of the Levy *et al.* (2014) model. The age-depth curve below the deepest age (i.e.,
168 before 10.2 ka) is extrapolated and very uncertain. Cosmogenic surface exposure dating
169 indicates that the landscape surrounding the lake was deglaciated by 10.7 ka (Levy *et al.* 2014),
170 and may be most consistent with the younger end (i.e., ~11 ka) of the range of ages for onset of
171 lacustrine sedimentation suggested by the age model. Confidence ranges (95% confidence) for
172 the remainder of the age model vary from 200 years during the middle Holocene, which was
173 more densely sampled for ^{14}C , to 600 years near the bottom-most ages (see the gray envelope in
174 Fig. 4). Therefore, ages stated below should be considered to have uncertainties of at least ± 100
175 to 300 years, depending upon their position in the record.

176

177 *Palaeoenvironmental proxy data*

178 The early postglacial.

179 The oldest lake sediments at LCL, which overlie diamicton (Levy *et al.* 2014) and date to
180 sometime prior to 10 ka, contain assemblages dominated by *Oliveridia/Hydrobaenus* and by
181 Tanytarsini including *Micropsectra* (Fig. 5). Some Tanytarsini may be pioneering postglacial

1
2
3
4
5
6
7
8
9
10
11
12
13
14
15
16
17
18
19
20
21
22
23
24
25
26
27
28
29
30
31
32
33
34
35
36
37
38
39
40
41
42
43
44
45
46
47
48
49
50
51
52
53
54
55
56
57
58
59
60

colonizers of arctic lakes (Saulnier-Talbot & Pienitz 2010; Axford *et al.* 2011), so succession may partly explain the composition of these assemblages. At the same time, several lines of evidence suggest that the period before 10 ka was characterized by low temperatures, dilute waters and low productivity: the cold stenotherm *Oliveridia/Hydrobaenus* was abundant; assemblages from this period are similar to those of the late Holocene at LCL and to modern assemblages from lakes ~650 km north on Store Koldewey (Schmidt *et al.* 2011); and OM and bioSiO₂ are very low in sediments from this period (<2% dry weight of each; Fig. 6).

The early to middle Holocene.

By 10 ka, *Oliveridia/Hydrobaenus* declined while Tanypodinae and *Psectrocladius* (both found in relatively nutrient-rich lakes and absent from more dilute, nutrient-poor lakes in West Greenland; Brodersen & Anderson 2002) became abundant. *Procladius*, which is associated in Arctic Canada with both relatively high temperatures and high dissolved organic carbon (Gajewski 2005) and was found in Duck and Hjort lakes on Store Koldewey only during the inferred local HTM (Schmidt *et al.* 2011), was consistently present at LCL from 10.1 to 3.6 ka. Combined with the onset of significant bioSiO₂ production and the jump to 10% OM abundance after 9.8 ka, this chironomid assemblage shift suggests a transition to warmer and more productive conditions.

The continuing rise of bioSiO₂ and OM throughout the subsequent millennia of inferred HTM warmth provides evidence for increasing lake and possibly landscape productivity throughout the HTM. Supporting this interpretation, *Psectrocladius* and *Cricotopus*, chironomid genera commonly associated with macrophytes and/or productive lakes (Brodersen *et al.* 2001; Langdon *et al.* 2010), experienced maximum abundances during the period of peak bioSiO₂ and

205 OM from ~7 to 4 ka. Sediment accumulation rates also rose above the overall (presumably
206 compaction-defined) Holocene trend during the period of peak bioSiO₂ and OM percentages
207 (Fig. 6).

208

209 Transition to the late Holocene.

210 Inferred temperatures began to decline in the middle Holocene by ~5.5 ka, followed more than
211 500 years later by a decline in bioSiO₂ and subsequently OM. An abrupt assemblage shift
212 occurred at ~3.5 ka, after which *Oliveridia/Hydrobaenus*, *Pseudodiamesa*, and *Micropsectra*
213 increased and Tanypodinae disappeared. BioSiO₂ and OM percentages were low after 3.5 ka,
214 both having values <10% for much of the past two millennia.

215

216 *Temperature modelling*

217 Quantitative temperature reconstructions generated using the three different models described
218 above show important differences and similarities (Fig. 5). The tolerance-downweighted WA
219 (FRA06) models are more sensitive to the presence of low abundances of cold stenotherms
220 (which by definition have narrow temperature tolerances in the training sets), as seen in two
221 samples ~9 and 7 ka. Reconstructions using FRA06 are indeed sensitive to our treatment of
222 *Psectrocladius* and Tanypodinae, with inclusion of those taxonomically ambiguous groups
223 yielding warmer temperature reconstructions in the early and middle Holocene. The FOR15
224 model yielded more stable inferred temperatures during the early and middle Holocene and
225 overall lower absolute temperatures. The decrease in temperatures inferred with FOR15 in the
226 last two millennia – not seen in reconstructions from FRA06, but consistent with a rise in the
227 cold stenotherm *Hydrobaenus/Oliveridia* and with changes in productivity indicators (bioSiO₂

1
2
3
4
5
6
7
8
9
10
11
12
13
14
15
16
17
18
19
20
21
22
23
24
25
26
27
28
29
30
31
32
33
34
35
36
37
38
39
40
41
42
43
44
45
46
47
48
49
50
51
52
53
54
55
56
57
58
59
60

and OM) – likely reflects the inclusion of colder training set sites in FOR15 (as cold as 2.0 °C vs. 5.0 °C for FRA06). The FOR15 training set may be better suited to reconstructing colder-than-present temperatures at Mid- to High Arctic sites than the FRA06 training set, which lacks analogues for very cold fossil sites as described previously (Axford *et al.* 2009). When compared with the FOR15 training set using MAT, all but two fossil samples from LCL have good analogues (defined as SCD less than the 5th percentile within the training set), and only one fossil sample is a no-analogue assemblage (defined as SCD greater than the 10th percentile within the training set; Fig. 5). In contrast, when compared with the FRA06 training set most fossil samples have SCDs greater than the 5th percentile, and many greater than the 10th percentile within that smaller training set. This further suggests that FOR15 is a better fit to our fossil data, presumably due to the colder climate space and more numerous sites represented in this training set.

Despite model differences, reconstructed millennial-scale temperature trends are similar between models, and most of the absolute temperature reconstructions are within sample-specific errors of one another (Fig. 5). Reflecting the similar trends indicated by the three models, they yielded similar reconstructed temperature anomalies, especially FOR15 compared with the FRA06-TR model excluding two taxonomically ambiguous groups (Fig. 6). We henceforth discuss anomalies rather than absolute temperature inferences, and furthermore we give greatest weight to inferences from the FOR15 training set, which as discussed above contains better analogues for our fossil data. July temperatures inferred from FOR15 were 3 to 4 °C higher from ~10 to 5.5 ka than in the last millennium, and anomalies inferred using the two FRA06 models generally bracket those estimates. The corresponding inferred overall rate of Neoglacial cooling, averaged over the period from 5.5 to 0.5 ka, was 0.6 to 0.8 °C per thousand years.

251

252 **Discussion**

253

254 *Interpreting chironomid assemblage shifts*

255 Aquatic ecosystems are sensitive to factors other than temperature – for example, vegetation

256 change and changes in water chemistry that may be associated with watershed ontogeny or

257 eutrophication from external nutrient sources (Anderson *et al.* 2008; Heggen *et al.* 2010;258 Kaufman *et al.* 2012; Luoto *et al.* 2015). Such secondary gradients may confound chironomid-259 based palaeotemperature reconstructions (Velle *et al.* 2005, 2010; cf. Brooks *et al.* 2012), and

260 must be considered as possible alternative drivers of midge assemblage changes. We note that

261 the sparsely vegetated, boulder-supported landscape surrounding LCL has almost no soil cover,

262 and that the regional arrival of *Betula nana* between 9 and 8 ka and regional but likely not local263 establishment of dwarf shrub tundra (Funder, 1978; Cremer *et al.* 2001) – the most significant

264 Holocene vegetation change in the region – does not coincide with a notable chironomid

265 assemblage shift at our study site. Although, as described above, some chironomid taxa

266 including *Psectrocladius* and *Cricotopus* may have responded to changes in macrophyte

267 abundance or other aspects of lake productivity, shifts in overall productivity and substrate

268 recorded by OM and bioSiO₂ do not predict shifts in inferred temperature. Rather, changes in

269 these variables consistently lag inferred temperature changes, as would be expected if past

270 millennial-scale temperature changes drove changes in lake trophic status. Thus we suggest that

271 secondary gradients do not seriously confound temperature reconstructions at this site.

272 Several additional observations lend confidence in modeled palaeotemperature trends at

273 LCL: Inferred temperature trends agree well between models (Fig. 6) – a necessary albeit not

1
2
3
4
5
6
7
8
9
10
11
12
13
14
15
16
17
18
19
20
21
22
23
24
25
26
27
28
29
30
31
32
33
34
35
36
37
38
39
40
41
42
43
44
45
46
47
48
49
50
51
52
53
54
55
56
57
58
59
60

sufficient test of model success. Qualitative interpretations based upon shifts in major taxa, discussed above, agree well with the quantitative reconstructions. Multiple indicators of relatively warm, productive conditions (e.g., *Procladius*, *Psectrocladius*) are abundant throughout the inferred early to middle Holocene thermal maximum, and multiple cold indicators (e.g., *Pseudodiamesa*, *Oliveridia/Hydrobaenus*; Fig. 6) replace them in the late Holocene. And importantly, as summarized below, the timings of inferred temperature changes also agree well with nearby independent palaeoclimate archives.

Evidence for the fidelity of chironomids as indicators of palaeotemperature at LCL agrees with previous studies concluding that temperature was likely the primary driver (in some cases probably via intermediary effects on lake chemistry and trophic status) of chironomid assemblage shifts in East Greenland through the Holocene (Wagner *et al.* 2005; Schmidt *et al.* 2011). In another relevant study, Medeiros *et al.* (2015) concluded that secondary gradients are relatively unproblematic in chironomid-based temperature reconstructions from unproductive Arctic lakes. Brooks *et al.* (2012) emphasized the importance of identifying *a priori* which site types are best suited to the use of chironomids as a palaeotemperature proxy. We postulate that sites like LCL with little soil or vegetation development through the Holocene, and probably relatively simple food webs, have especially strong potential for the use of chironomid assemblages to infer Holocene temperature shifts by minimizing the effects of many secondary gradients.

Holocene temperature change in East Greenland

We infer the highest temperatures in central East Greenland from ~10 to 5.5 ka, with average July air temperature anomalies of 3 to 4 °C relative to the last millennium of the Holocene (Fig.

6). Gradual cooling began by 5.5 ka in the middle Holocene, followed by additional assemblage shifts suggesting intensified cooling at ~4 to 3.5 ka and then progressively colder conditions throughout the late Holocene. Results from Two Move Lake, <0.5 km away, support these climatic interpretations: Influx of meltwater from nearby Bregne Ice Cap ceased at 10 ka when the ice cap retreated outside the lake's watershed, supporting the onset of warmer-than-present conditions at that time. Subsequent cooling is inferred from increasing non-glacial clastic sedimentation beginning at 6.5 ka, and glacial meltwater returned to the watershed initially at 2.6 ka and consistently after 1.9 ka as the ice cap expanded (Fig. 6; Levy *et al.* 2014).

The timing of peak warmth inferred from these two lakes is very similar to that inferred from sediment geochemistry, diatoms and chironomids at lakes Basaltsø and B1 on Geographical Society Ø ~230 km to the northeast (Fig. 1; Cremer *et al.* 2001; Wagner *et al.* 2005), and aligns with evidence for extralimital thermophilous marine bivalve species in and near Scoresby Sund ~9.5 to 6 ka (Hjort & Funder, 1974; Bennike & Wagner 2013). These studies add support to diverse evidence from land and sea for summer warmth in East Greenland during parts of the early and middle Holocene, and that Neoglacial cooling and its environmental impacts intensified within the late Holocene (e.g., Funder, 1978; Andrews *et al.* 1997; Jennings *et al.* 2002; Vinther *et al.* 2009; Schmidt *et al.* 2011; Lowell *et al.* 2013).

Evidence that warmer-than-present HTM conditions began as early as 10 ka at LCL and Two Move Lake contrasts with some records from East Greenland where the inferred onset of warmth came later, particularly at sites farther north (Schmidt *et al.* 2011; Wagner & Bennike 2015; Gajewski 2015). However, early warmth is supported by local precipitation isotopes over nearby Renland ice cap, where inferred temperatures consistently exceeded those of the last millennium for the first time at ~10 ka (Fig. 6; Vinther *et al.* 2009). Also nearby, 125 km east of

1
2
3
4
5
6
7
8
9
10
11
12
13
14
15
16
17
18
19
20
21
22
23
24
25
26
27
28
29
30
31
32
33
34
35
36
37
38
39
40
41
42
43
44
45
46
47
48
49
50
51
52
53
54
55
56
57
58
59
60

LCL, lakes adjacent to Istorvet ice cap experienced non-glacial sedimentation from ~9.7 to 0.9 ka (Lusas *et al.* 2011; Lowell *et al.* 2013). Warmth beginning ~10 ka suggests that by then any regional factors modulating the climatic response to insolation (e.g., effects of the waning but still proximal Greenland Ice Sheet on local energy balance, or the hypothesized atmospheric or oceanic effects of continuing Laurentide deglaciation; Kaufman *et al.* 2004; Kaplan & Wolfe 2006; Renssen *et al.* 2009) did not override the effects of enhanced insolation forcing around inner Scoresby Sund.

The average, overall rate of Neoglacial summer cooling inferred here for central East Greenland between 5.5 and 0.5 ka (0.6 to 0.8 °C per thousand years) is at least twice that estimated for late Holocene summers across the Arctic as a whole (Kaufman *et al.* 2009). Recent palaeodata syntheses and modelling studies alike support the notion that there were strong and complex spatial variations in the magnitude, seasonality, and probably timing of peak HTM warmth around the Arctic and subarctic (Renssen *et al.* 2009, 2012; Zhang *et al.* 2010; Marcott *et al.* 2013; Briner *et al.* 2016; Kaufman *et al.* 2016). Our results suggest that central East Greenland experienced a larger summer temperature anomaly during the HTM than some other parts of the Arctic, perhaps due to especially strong positive feedbacks from sea ice or other local factors.

The HTM summer temperature anomaly reconstructed at LCL also exceeds the annually integrated anomalies inferred from oxygen isotopes in the Renland ice core and from borehole temperatures at GRIP to the west on the Greenland Ice Sheet (Dahl-Jensen *et al.* 1998; Vinther *et al.* 2009), and the overall rate of Neoglacial cooling at LCL exceeds that inferred from argon and nitrogen isotopes in trapped air bubbles through the late Holocene at GISP2 (Kobashi *et al.* 2011). This may be explained in whole or part by the differing seasonal biases of these records,

combined with altered seasonality of HTM climate driven by a positive summer (and slightly negative winter) insolation anomaly.

Together, all of these results illustrate the importance of local, seasonally specific temperature reconstructions in accurately characterizing climates of the past. Given the utility of HTM palaeoclimate data as targets for improving climate and ice sheet models (Simpson *et al.* 2009; Applegate *et al.* 2012; Lecavalier *et al.* 2014), and the important role of summer temperatures at low elevations in driving ice sheet mass balance, it should be a priority to further elucidate the magnitude and seasonality of past warmth around the margins of the Greenland Ice Sheet.

Conclusions

Chironomid assemblage shifts track temperature through the Holocene at Last Chance Lake in central East Greenland. At this site near inner Scoresby Sund and Renland ice cap, the timing of chironomid-inferred temperature shifts is in good agreement with nearby ice core and glacial geological evidence, and reconstructed temperature trends throughout the Holocene agree well between our chironomid-based models. We have argued that sites with similarly minimal soil and vegetation development through the Holocene may be especially well suited to the use of chironomids for inferring Holocene temperatures, because they are less affected by some important, potentially confounding secondary gradients.

Warmest Holocene conditions were registered in central East Greenland ~10 to 5.5 ka, with July air temperature anomalies of 3 to 4 °C relative to the preindustrial last millennium. The early onset of intense warming here argues against a cooling effect on local climate from the

1
2
3
4
5
6
7
8
9
10
11
12
13
14
15
16
17
18
19
20
21
22
23
24
25
26
27
28
29
30
31
32
33
34
35
36
37
38
39
40
41
42
43
44
45
46
47
48
49
50
51
52
53
54
55
56
57
58
59
60

366 melting Laurentide Ice Sheet, as has been proposed for some sites in the northwestern North
367 Atlantic region. This site experienced gradual cooling after ~5.5 ka, and progressively colder
368 conditions after ~4 to 3.5 ka. The estimated rate of Neoglacial cooling in central East Greenland,
369 averaged over the period from 5.5 to 0.5 ka, was 0.6 to 0.8 °C per thousand years. Neoglacial
370 cooling here occurred at more than twice the rate estimated for the Arctic as a whole, suggesting
371 significant spatial variability in the magnitude of the temperature response to insolation forcing
372 across the Arctic.

373

374 Acknowledgements. This work was partly funded by the U.S. NSF (ARC-0909270 to Kelly,
375 ARC-0909285 to Lowell, ARC-0908081 to Hall, ARC-1454734 to Axford) and the Institute for
376 Sustainability and Energy at Northwestern University (ISEN). C. Carrio and G. Schellinger
377 made chironomid identifications, with input from J. McFarlin. S. Hammer and L. Hempel
378 assisted in the lab. Biogenic silica was measured in the Sedimentary Records of Environmental
379 Change Laboratory at Northern Arizona University. Staff at the National Lacustrine Core
380 Facility (LacCore) assisted with processing sediment cores. ¹⁴C was measured at the National
381 Ocean Sciences Accelerator Mass Spectrometry (NOSAMS) facility. B. Honsaker and A. R.
382 Lusas assisted in the field. This work benefited from use of the training set data of Fortin *et al.*
383 (2015), made publically available by M.-C. Fortin, A.S. Medeiros and collaborators via the
384 Canadian Cryospheric Information Network’s Polar Data Catalogue. Anonymous reviewers are
385 thanked for their thoughtful feedback on our manuscript.

387 REFERENCES

- Anderson, N. J., Brodersen, K. P., Ryves, D. B., McGowan, S., Johansson, L. S., Jeppesen, E. & Leng, M. J. 2008: Climate versus in-lake processes as controls on the development of community structure in a low-arctic lake (South-West Greenland). *Ecosystems* 11, 307–324.
- Andrews, J. T., Smith, L. M., Preston, R., Cooper, T. & Jennings, A. E. 1997: Spatial and temporal patterns of iceberg rafting (IRD) along the East Greenland margin, ca 68 degrees N, over the last 14 cal ka. *Journal of Quaternary Science* 12, 1–13.
- Applegate, P. J., Kirchner, N., Stone, E. J., Keller, K. & Greve, R. 2012: An assessment of key model parametric uncertainties in projections of Greenland Ice Sheet behavior. *The Cryosphere* 6, 589–606.
- Axford, Y., Briner, J. P., Francis, D. R., Miller, G. H., Walker, I. R. & Wolfe, A. P. 2011: Chironomids record terrestrial temperature changes throughout arctic interglacials of the past 200,000 years. *Geological Society of America Bulletin* 123, 1275–1287.
- Axford, Y., Briner, J. P., Miller, G. H. & Francis, D. R. 2009: Paleoecological evidence for abrupt cold reversals during peak Holocene warmth on Baffin Island, Arctic Canada. *Quaternary Research* 71, 142–149.
- Axford, Y., Losee, S., Briner, J. P., Francis, D. R., Langdon, P. G. & Walker, I. R. 2013: Holocene temperature history at the western Greenland Ice Sheet margin reconstructed from lake sediments. *Quaternary Science Reviews* 59, 87–100.
- Bennike, O. & Wagner, B. 2013: Holocene range of *Mytilus edulis* in central East Greenland. *Polar Record* 49, 291–296.
- Blaauw, M. 2010: Methods and code for 'classical' age-modelling of radiocarbon sequences. *Quaternary Geochronology* 5, 512–518.
- Briner, J. P., McKay, N., Axford, Y., Bennike, O., Bradley, R. S., de Vernal, A., Fisher, D., Francus, P., Frechette, B., Gajewski, K., Jennings, A., Kaufman, D. S., Miller, G., Rouston, C. & Wagner, B. 2016: Holocene climate change in Arctic Canada and Greenland. *Quaternary Science Reviews* 147, 340–364.
- Brodersen, K. P. & Odgaard, B. V., Vestergaard, O., Anderson, N. J. 2001: Chironomid stratigraphy in the shallow and eutrophic Lake Søbygaard, Denmark: chironomid-macrophyte co-occurrence. *Freshwater Biology* 45, 253–267.
- Brodersen, K. P. & Anderson, N. J. 2002: Distribution of chironomids (Diptera) in low arctic West Greenland lakes: trophic conditions, temperature and environmental reconstruction. *Freshwater Biology* 47, 1137–1157.
- Brooks, S. J., Langdon, P. G. & Heiri, O. 2007: The Identification and Use of Palearctic Chironomidae Larvae in Palaeoecology. *Quaternary Research Association Technical Guide 10*. Quaternary Research Association, 276 pp.
- Brooks, S. J., Axford, Y., Heiri, O., Langdon, P. G. & Larocque-Tobler, I. 2012: Chironomids can be reliable proxies for Holocene temperatures. A comment on Velle et al. (2010). *The Holocene* 22, 1495–1500.
- Cartensen, L. S. & Jørgensen, B. V. 2009: Weather and Climate Data from Greenland 1958–2008. *Technical Report 09-11*. Ministry of Climate and Energy, Copenhagen, 22 pp.

- 431 Cremer, H., Melles, M. & Wagner, B. 2001: Holocene climate changes reflected in a diatom
432 succession from Basaltsø, East Greenland. *Canadian Journal of Botany* 79, 649-656.
- 433 Dahl-Jensen, D., Mosegaard, K., Gundestrup, N., Clow, G. D., Johnsen, S. J., Hansen & A. W.,
434 Balling, N. 1998: Past temperatures directly from the Greenland ice sheet. *Science* 282,
435 268-271.
- 436 D'Andrea, W. J., Huang, Y., Fritz, S. C. & Anderson, N. J. 2011: Abrupt Holocene climate
437 change as an important factor for human migration in West Greenland. *Proceedings of*
438 *the National Academy of Sciences* 108, 9765-9769.
- 439 Eggermont, H. & Heiri, O. 2011: The chironomid-temperature relationship: expression in nature
440 and palaeoenvironmental implications. *Biological Reviews* 87, 430-456.
- 441 Fortin, M-C., Medeiros, A. S., Gajewski, K., Barley, E. M., Larocque-Tobler, I., Porinchu, D. F.
442 & Wilson, S. E. 2015: Chironomid-environment relations in northern North America.
443 *Journal of Paleolimnology* 54, 223-237.
- 444 Francis, D., Wolfe, A., Walker, I. & Miller, G. 2006: Interglacial and Holocene temperature
445 reconstructions based on midge remains in sediments of two lakes from Baffin Island,
446 Nunavut, Arctic Canada. *Palaeogeography, Palaeoclimatology, Palaeoecology* 236, 107-
447 124.
- 448 Fréchette, B. & de Vernal, A. 2009: Relationship between Holocene climate variations over
449 southern Greenland and eastern Baffin Island and synoptic circulation pattern. *Climate of*
450 *the Past* 5, 347-359.
- 451 Funder, S. 1978: Holocene stratigraphy and vegetation history in the Scoresby Sund area, East
452 Greenland. *Grønlands Geologiske Undersøgelse Bulletin* 129, 66 pp.
- 453 Funder, S., Goose, H., Jepsen, H., Kaas, E., Kjaer, K. H., Korsgaard, N. J., Larsen, N. K.,
454 Linderson, H., Lysa, A., Moller, P., Olsen, J. & Willerslev, E. 2011: A 10,000-year
455 record of arctic Ocean sea-ice variability – View from the beach. *Science* 333, 747-750.
- 456 Gajewski, K., Bouchard, G., Wilson, S. E., Kurek, J. & Cwynar, L. C. 2005: Distribution of
457 Chironomidae (Insecta: Diptera) head capsules in recent sediments of Canadian Arctic
458 lakes. *Hydrobiologia* 549, 131-143.
- 459 Gajewski, K. 2015: Quantitative reconstruction of Holocene temperatures across the Canadian
460 Arctic and Greenland. *Global and Planetary Change* 128, 14-23.
- 461 Heggen, M. P., Birks, H. H. & Anderson, N. J. 2010: Long-term ecosystem dynamics of a small
462 lake and its catchment in West Greenland. *The Holocene* 20, 1207-1222
- 463 Heiri, O., Lotter, A. F. & Lemcke, G. 2001: Loss on ignition as a method for estimating organic
464 and carbonate content in sediments: Reproducibility and compatibility of results. *Journal*
465 *of Paleolimnology* 25, 101-110.
- 466 Hjort, C. & Funder, S. 1974: The subfossil occurrence of *Mytilus edulis* L. in central East
467 Greenland. *Boreas* 3, 23-33.
- 468 Jennings, A. E., Knudsen, K. L., Hald, M., Hansen, C. V. & Andrews, J. T. 2002: A mid
469 Holocene shift in Arctic sea-ice variability on the East Greenland Shelf. *The Holocene*
470 12, 49-58.

- Johnsen, S. J., Dahl-Jensen, D., Gundestrup, N., Steffensen, J. P., Clausen, H. B., Miller, H., Masson-Delmotte, V., Sveinbjornsdóttir, A. E. & White, J. 2001: Oxygen isotope and palaeotemperature records from six Greenland ice-core stations: Camp Century, Dye-3, GRIP, GISP2, Renland and NorthGRIP. *Journal of Quaternary Science* 16, 299-307.
- Kaplan, M. R. & Wolfe, A. P. 2006: Spatial and temporal variability of Holocene temperature in the North Atlantic region. *Quaternary Research* 65, 223-231.
- Kaufman, D. S., Ager, T. A., Anderson, N. J., Anderson, P. M., Andrews, J. T., Bartlein, P. J., Brubaker, L. B., Coats, L. L., Cwynar, L. C., Duval, M. L., Dyke, A. S., Edwards, M. E., Eisner, W. R., Gajewski, K., Geirsdóttir, A., Hu, F. S., Jennings, A. E., Kaplan, M. R., Kerwin, M. W., Lozhkin, A. V., MacDonald, G. M., Miller, G. H., Mock, C. J., Oswald, W. W., Otto-Bliesner, B. L., Porinchu, D. F., Rühland, K., Smol, J. P., Steig, E. J. & Wolfe, B. B. 2004: Holocene thermal maximum in the western Arctic (0-180° W). *Quaternary Science Reviews* 23, 529-560.
- Kaufman, D. S., Anderson, R. S., Axford, Y., Lamoureux, S., Schindler, D., Walker, I. R. & Werner, A. 2012: A multi-proxy record of the Last Glacial Maximum and last 14,500 years of paleo-environmental change at Lone Spruce Pond, southwestern Alaska. *Journal of Paleolimnology* 48, 9-26.
- Kaufman, D. S., Axford, Y., Henderson, A. C. G., McKay, N. P., Oswald, W. W., Saenger, C., Anderson, R. S., Bailey, H. L., Clegg, B., Gajewski, K., Hu, F. S., Jones, M. C., Massa, C., Routson, C. C., Werner, A., Wooller, M. J. & Yu, Z. 2016: Holocene climate changes in eastern Beringia (NW North America) – a systematic review of multi-proxy evidence. *Quaternary Science Reviews* 147, 312-339.
- Kaufman, D. S., Schneider, D. P., McKay, N. P., Ammann, C. M., Bradley, R. S., Briffa K. R., Miller, G. H., Otto-Bliesner, B. L., Overpeck, J. T., Vinther, B. M. & Arctic Lakes 2k Project Members (Abbott, M., Axford, Y., Bird, B., Birks, H. J. B., Bjune, A. E., Briner, J., Cook, T., Chipman, M., Francus, P., Gajewski, K., Geirsdóttir, Á., Hu, F. S., Kutchko, B., Lamoureux, S., Loso, M., MacDonald, G., Peros, M., Porinchu, D., Schiff, C., Seppä, H. & Thomas, E.). 2009: Recent warming reverses long-term Arctic cooling. *Science* 325, 1236-1239.
- Kobashi, T., Kawanura, K., Severinghaus, J. P., Barnola, J-M., Nakaegawa, T., Vinther, B. M., Johnsen, S. J. & Box, J. E. 2011: High variability of Greenland surface temperature over the past 4000 years estimated from trapped air in an ice core. *Geophysical Research Letters* 38, L21501.
- Langdon, P. G., Ruiz, Z., Wynee, S., Sayer, C. D. & Davidson, T. A. 2010: Ecological influences on larval chironomid communities in shallow lakes: implications for palaeolimnological interpretations. *Freshwater Biology* 55, 531-545.
- Larsen, N. K., Kjaer, K. H., Lecavalier, B., Bjork, A. A., Colding, S., Huybrechts, P., Jakobsen, K. E., Kjeldsen, K. K., Knudsen, K-L., Odgaard, B. V. & Olsen, J. 2015: The response of the southern Greenland ice sheet to the Holocene thermal maximum. *Geology* 43, 291-294.
- Lecavalier, B. S., Milne, G. A., Simpson, M. J. R., Wake, L., Huybrechts, P., Tarasov, L., Kjeldsen, K., Funder, S., Long, A. J., Woodroffe, S., Dyke, A. S. & Larsen, N. K. 2014: A

- 513 model of Greenland ice sheet deglaciation constrained by observations of relative sea
514 level and ice extent. *Quaternary Science Reviews* 102, 54-84.
- 515 Levy, L. B., Kelly, M. A., Lowell, T. V., Hall, B. L., Hempl, L. A., Honsaker, W. M., Lusas, A.
516 R., Howley, J. A. & Axford, Y. 2014: Holocene glacier fluctuations near the eastern
517 margin of the Greenland Ice Sheet, Bregne ice cap, Scoresby Sund, eastern Greenland.
518 *Quaternary Science Reviews* 92, 357-368.
- 519 Lowell, T. V., Hall, B. L., Kelly, M. A., Bennike, O., Lusas, A. R., Honsaker, W., Smith, C. A.,
520 Levy, L. B., Travis, S. & Denton, G. H. 2013: Late Holocene expansion of Istorvet ice
521 cap, Liverpool Land, east Greenland. *Quaternary Science Reviews* 63, 128-140.
- 522 Luoto, T. P., Oksman, M. & Ojala A. E. K. 2015: Climate change and bird impacts as drivers of
523 High Arctic pond deterioration. *Polar Biology* 38, 357-368.
- 524 Lusas, A. R. 2011: *Holocene Fluctuations of Istorvet Ice Cap, Liverpool Land, East Greenland*.
525 M. Sc. thesis, University of Maine, 135 pp.
- 526 Medeiros, A. S., Gajewski, K., Porinchu, D. F., Vermaire, J. C. & Wolfe, B. B. 2015: Detecting
527 the influence of secondary environmental gradients in chironomid-inferred
528 paleotemperature reconstructions in northern North America. *Quaternary Science*
529 *Reviews* 124, 265-274.
- 530 Marcott, S. A., Shakun, J. D., Clark, P. U. & Mix, A. C. 2013: A reconstruction of regional and
531 global temperature for the past 11 300 years. *Science* 339, 1198-1201.
- 532 Mortlock, R. A. & Froelich, P. N. 1989: A simple method for the rapid determination of biogenic
533 opal in pelagic marine sediments. *Deep-Sea Research Part A* 36, 1415-1426.
- 534 Reimer, P. J., Bard, E., Bayliss, A., Beck, J. W., Blackwell, P. G., Bronk Ramsey, C., Buck, C.
535 E., Edwards, R. L., Friedrich, M., Grootes, P. M., Guilderson, T. P., Haflidason, H.,
536 Hajdas, I., Hatté, C., Heaton, T. J., Hoffmann, D. L., Hogg, A. G., Hughen, K. A., Kaiser,
537 K. F., Kromer, B., Manning, S. W., Niu, M., Reimer, R. W., Richards, D. A., Scott, E.
538 M., Southon, J. R., Turney, C. S. M. & van der Plicht, J. 2013: IntCal13 and Marine13
539 radiocarbon age calibration curves, 0-50,000 years cal BP. *Radiocarbon* 55, 1869-1887.
- 540 Renssen, H., Seppä, H., Heiri, O., Roche, D. M., Goosse, H. & Fichet, T. 2009: The spatial and
541 temporal complexity of the Holocene thermal maximum. *Nature Geoscience* 2, 410-413.
- 542 Renssen, H., Seppä, H., Crosta, X., Goosse, H. & Roche, D. M. 2012: Global characterization of
543 the Holocene Thermal Maximum. *Quaternary Science Reviews* 48, 7-19.
- 544 Saulnier-Talbot, É. & Pienitz, R. 2010: Postglacial chironomid assemblage succession in
545 northernmost Ungava Peninsula, Canada. *Journal of Quaternary Science* 25, 203-213.
- 546 Schmidt, S., Wagner, B., Heiri, O., Klug, M., Bennike, O. & Melles, M. 2011: Chironomids as
547 indicators of the Holocene climatic and environmental history of two lakes in Northeast
548 Greenland. *Boreas* 40, 116-130.
- 549 Simpson, M. J. R., Milne, G. A., Huybrechts, P. & Long, A. J. 2009: Calibrating a glaciological
550 model of the Greenland ice sheet from the Last Glacial Maximum to present-day using
551 field observations of relative sea level and ice extent. *Quaternary Science Reviews* 28,
552 1631-1657.

- Sundqvist, H. S., Kaufman, D. S., McKay, N. P., Balascio, N. L., Briner, J. P., Cwynar, L. C., Sejrup, H. P., Seppä, H., Subetto, D. A., Andrews, J. T., Axford, Y., Bakke, J., Birks, H. J. B., Brooks, S. J., de Vernal, A., Jennings, A. E., Ljungqvist, F. C., Rühland, K. M., Saenger, C., Smol, J. P. & Viau, A. E. 2014: Arctic Holocene proxy climate database – New approaches to assessing geochronological accuracy and encoding climate variables. *Climate of the Past* 10, 1-63.
- Velle, G., Brodersen, K. P., Birks, H. J. B. & Willassen, E. 2010: Midges as quantitative temperature indicator species: Lessons for palaeoecology. *The Holocene* 20, 989-1002.
- Velle, G., Brooks, S. J., Birks, H. J. B. & Willassen, E. 2005: Chironomids as a tool for inferring Holocene climate: an assessment based on six sites in southern Scandinavia. *Quaternary Science Reviews* 24, 1429-1462.
- Vinther, B. M., Buchardt, S. L., Clausen, H. B., Dahl-Jensen, D., Johnsen, S. J., Fisher, D. A., Koerner, R. M., Raynaud, D., Lipenkov, V., Andersen, K. K., Blunier, T., Rasmussen, S. O., Steffensen, J. P. & Svensson, A. M. 2009: Holocene thinning of the Greenland ice sheet. *Nature* 461, 385-388.
- Wagner, B., Heiri, O. & Hoyer, D. 2005: Chironomids as proxies for palaeoenvironmental changes in East Greenland: a Holocene record from Geographical Society Ø. *Zeitschrift der Deutschen Geologischen Gesellschaft* 156, 543–556.
- Wagner, B. & Bennike, O. 2015: Holocene environmental change in the Skallingen area, eastern North Greenland, based on a lacustrine record. *Boreas* 44, 45–59.
- Walker, I. R. 2001: Midges: Chironomidae and related Diptera. In Smol, J. P., Birks, H. J. B. & Last, W. M. (eds.): *Tracking Environmental Change Using Lake Sediments. Volume 4: Zoological Indicators*, 43-66, Kluwer, Dordrecht.
- Walker, I. R., Smol, J. P., Engstrom, D. R. & Birks, H. J. B. 1991: An assessment of Chironomidae as quantitative indicators of past climatic change. *Canadian Journal of Fisheries and Aquatic Sciences* 48, 975-987.
- Walker, M. J. C., Berkelhammer, M., Björck, S., Cwynar, L. C., Fisher, A., Long, A. J., Lowe, J. L., Newnham, R. M., Rasmussen, S. O. & Weiss, H. 2012: Formal subdivision of the Holocene Series/Epoch: a Discussion Paper by a Working Group of INTIMATE (Integration of ice-core, marine and terrestrial records) and the Subcommittee on Quaternary Stratigraphy (International Commission on Stratigraphy). *Journal of Quaternary Science* 27, 649-659.
- Wiederholm, T. 1983: Chironomidae of the Holarctic Region. Keys and Diagnoses: Part 1. Larvae. *Entomologica Scandinavica Supplement* 19, 457 pp.
- Wooller, M. J., Francis, D., Fogel, M. L., Miller, G. H., Walker, I. R. & Wolfe, A. P. 2004: Quantitative paleotemperature estimates from $\delta^{18}\text{O}$ of chironomid head capsules preserved in arctic lake sediments. *Journal of Paleolimnology* 31, 267-274.
- Zhang, Q., Sundqvist, H. S., Moberg, A., Kornich, H., Nilsson, J. & Holmgren, K. 2010: Climate change between the mid and late Holocene in northern high latitudes – Part 2: Model-data comparisons. *Climate of the Past* 6, 609-626.

1
2
3
4
5
6
7
8
9
10
11
12
13
14
15
16
17
18
19
20
21
22
23
24
25
26
27
28
29
30
31
32
33
34
35
36
37
38
39
40
41
42
43
44
45
46
47
48
49
50
51
52
53
54
55
56
57
58
59
60

Figures

Fig. 1. Map of Greenland (A) and the Scoresby Sund region (inset, B) showing location of Last Chance Lake and other geographic features mentioned in the text. Gray shading denotes present-day ice cover.

Fig. 2. Photograph of Last Chance Lake (in foreground, with boat used for coring in August 2010). View is toward the southeast.

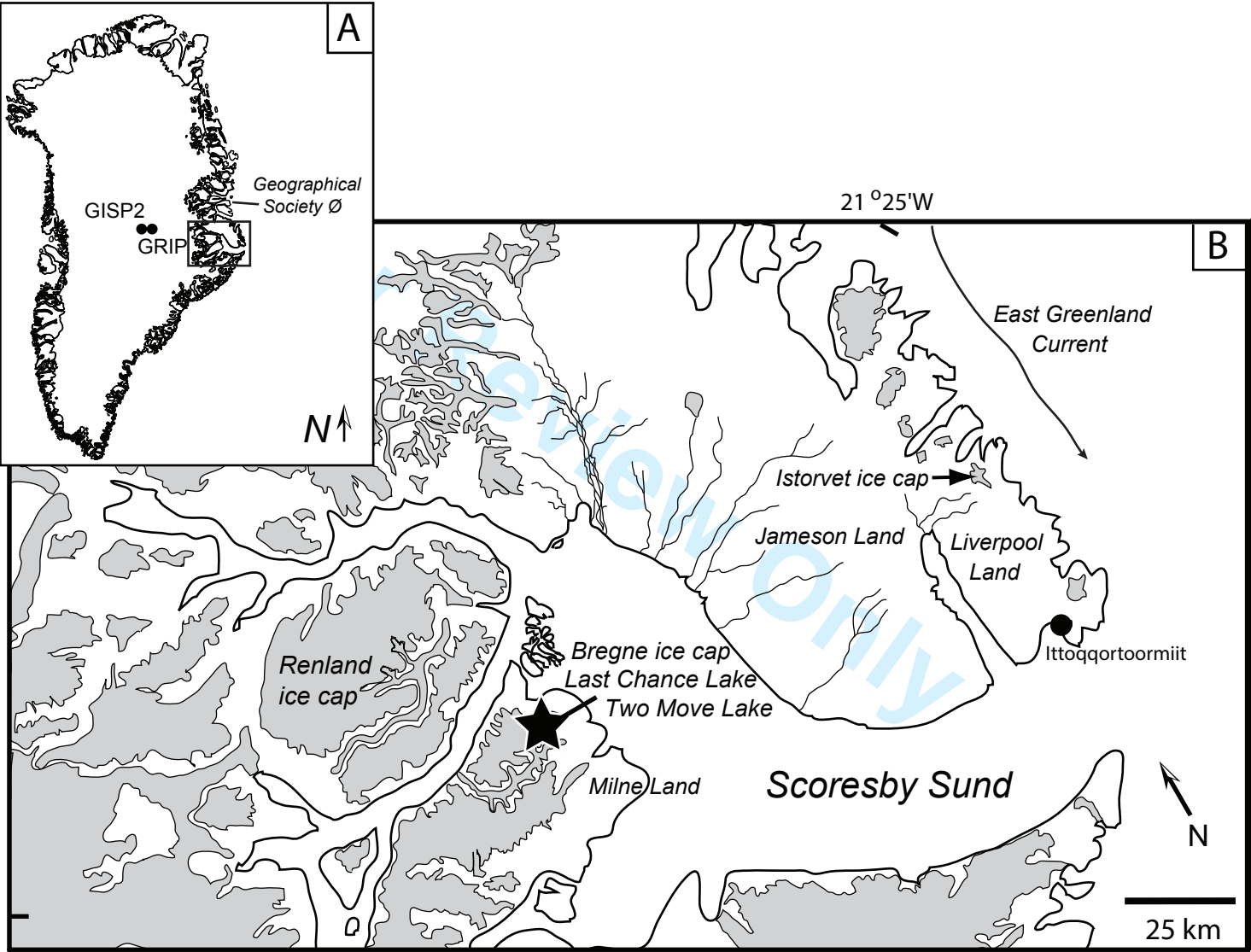
Fig. 3. Head capsule of *Psectrocladius nr barbimanus* morphotype (authors' informal designation). Photo by G. Schellinger, Northwestern University.

Fig. 4. Age-depth model for Last Chance Lake lacustrine sediments. Blue bands show 95% probability (highest posterior density) ranges of calibrated ¹⁴C ages, and gray zone shows 95% confidence intervals of the smooth spline. The age at 56.25 cm depth was excluded from the model, as was the underlying diamicton unit (from 83.5-75.5 cm depth, interpreted as till by Levy *et al.* 2014).

Fig. 5. Chironomid data from Last Chance Lake, including count sums (vertical line indicates value of 50), chironomid-inferred absolute July air temperatures, percent abundances of chironomid taxa (unfilled lines indicate 5× exaggeration) and squared chord distances (SCD) to nearest training set analogues. Reconstructions are based upon three different inference models, as described in the text: the WA model of Francis *et al.* (2006; FRA06), plus a variant with taxa

1
2
3 617 removed (FRA06-TR), and the WA-PLS model of Fortin *et al.* (2015; FOR15). Bootstrapped
4
5
6 618 sample-specific errors for two models are shown. Dotted lines on SCD plots show 5th and 10th
7
8 619 percentiles within the respective training sets. For temperature reconstructions expressed as
9
10 620 anomalies, see Fig. 6.
11
12
13 621
14 622 Fig. 6. (A) Multi-proxy results from Last Chance Lake, including modeled age-depth
15
16 623 relationship (with ^{14}C ages plotted as squares), sediment accumulation rates (SAR), weight
17
18 624 percents organic matter (OM) and biogenic silica (bioSiO_2), and chironomid-inferred July air
19
20 625 temperature anomalies (calculated relative to the preindustrial last millennium). This study's
21
22 626 updated age model is shown as a black line, and the original age model from Levy *et al.* (2014)
23
24 627 is shown as a green line; the two models are indistinguishable at this figure scale. Note that the
25
26 628 first-order trend in SAR likely reflects sediment compaction, as SAR values are not corrected for
27
28 629 density or water content. As discussed in the text, we give greatest weight to the FOR15
29
30
31
32 630 reconstruction (thick black line). (B) Palaeoclimate indicators from nearby Renland ice cap
33
34 631 (Vinther *et al.* 2009) and Two Move Lake (Levy *et al.* 2014).
35
36
37
38 632
39
40
41
42
43
44
45
46
47
48
49
50
51
52
53
54
55
56
57
58
59
60

1
2
3
4
5
6
7
8
9
10
11
12
13
14
15
16
17
18
19
20
21
22
23
24
25
26
27
28
29
30
31
32
33
34
35
36
37





254x166mm (300 x 300 DPI)

ew Only



169x169mm (300 x 300 DPI)

